



Research Article

Determination of the Activity Inventory in the Structural Components of the Dalat Nuclear Research Reactor for Its Decommissioning Planning

Quoc-Duong Tran, Kien-Cuong Nguyen , Ba-Vien Luong, Ton-Nghiem Huynh, Quang-Huy Pham, Doan-Hai-Dang Vo, and Nhi-Dien Nguyen 

Dalat Nuclear Research Institute, 01 Nguyen Tu Luc Str., Dalat City, Lam Dong 670000, Vietnam

Correspondence should be addressed to Nhi-Dien Nguyen; diennn.re@dnri.vn

Received 10 March 2022; Accepted 26 April 2022; Published 18 May 2022

Academic Editor: Peter Ivanov

Copyright © 2022 Quoc-Duong Tran et al. This is an open access article distributed under the Creative Commons Attribution License, which permits unrestricted use, distribution, and reproduction in any medium, provided the original work is properly cited.

This report presents the methods and calculated results of the activity inventory in the structural components of the Dalat Nuclear Research Reactor (DNRR). These components include the shielding concrete, the reactor tank, and its inside irradiated facilities; the thermal and thermalizing columns; and the horizontal channels. The MCNP5 code with a three-dimensional neutron transport model was used to calculate the neutron flux distribution, neutron energy spectrum at different locations, and activation cross sections of long-lived radioactive nuclides in activated major materials, including heavy concrete, reflection graphite, and aluminum of the reactor. The calculated results of the energy spectrum and activation cross sections of MCNP5 were used in the ORIGEN2.1 point depletion code to calculate the neutron-induced activity of activated materials at different time points by modeling the irradiation history and radioactive decay. Radioactivity of long-lived key activation products such as ^{41}Ca , ^{60}Co , ^{55}Fe , ^{63}Ni , and ^{152}Eu was modeled, and volumes of radioactive waste mainly of ordinary concrete, graphite, and aluminum in the structural components of the reactor were estimated. Experimental results of neutron flux and specific activities of some typical nuclides such as ^{60}Co , ^{152}Eu , ^{55}Fe , and ^{63}Ni in activated aluminum samples showed good agreement with the calculated results. As part of the national regulation requirements, the obtained data have been used to develop the decommissioning plan for the operational DNRR, with an estimation of about 10 years before its permanent shutdown.

1. Introduction

The Dalat Nuclear Research Reactor (DNRR), which has a nominal power of 500 kW, was reconstructed and upgraded from the US-made 250-kW pool-typed TRIGA Mark II reactor. Distilled light water is used as coolant, neutron moderator, reflector, and radiation shielding. After its reconstruction and upgrading, since March 1984, the reactor has been officially put into operation for the purposes of radioisotope production, neutron activation analysis, fundamental and applied research, and manpower training but without having a preliminary decommissioning plan [1–3].

As usual, decommissioning planning is required at the design stage and throughout the lifetime of a nuclear facility

[4]. The knowledge of decommissioning planning is required to choose the appropriate activation levels and amounts of radioactive decommissioning waste for the design of safe dismantling procedures. The activity inventories of different waste streams are also important for both the interim storage and final disposal of the decommissioning waste.

The objective of our study is to identify and evaluate the radioactive inventory of long-lived key activation products in the structural components of the operational DNRR for developing the decommissioning plan during its lifetime, following the safety requirements of the International Atomic Energy Agency (IAEA) guidelines, international practices, and relicensing requests. For decommissioning

TABLE 1: Main parameters of the DNRR structure components.

Structure component	Shape type	Parameters (cm)					Material
		Radius		Width	Length	Height	
		Inner	Outer				
Reactor tank	Cylindrical	99.4	100.0	—	—	625.0	Aluminum
Reactor core	Cylindrical	22.1		—	—	60.0	Aluminum, stainless steel, and fuel inside
Graphite reflector	Ring-shaped block	23.75	54.25	—	—	55.9	Graphite
Thermal column	Rectangular	—	—	120.0	160.0	120.0	Graphite
Biological shield	Octagonal	—	—	696.0	863.0	655.0	Steel-reinforced concrete

planning of operational research reactors, experimental data are limited due to samples for measurement that can be taken only with the components outside the reactor core, such as shielding concrete samples [5, 6], shielding concrete samples and neutron flux measurement [7], primary cooling system [8], or without any experiments [9]. For those reactors, a computational approach enables a nondestructive initial estimate, but systematic measurements are also needed to verify the calculated results. For research reactors scheduled to be permanently shut down and whose final decommissioning plans had been developed, samples were much easier to be taken from different structural components of the reactors, such as for analyzing the compositions and measuring radioactivity and dose rates at the outer area of the upper aluminum grid plate of the TRIGA reactor [10], for characterizing graphite and Flualent neutron moderator materials of the FIR1 TRIGA reactor [11, 12], and for radiological characterization of the VVR-S reactor block [13].

Different computer codes can be used to model the neutron flux values and flux shapes, reaction rate, etc. For example, the two-dimensional SN method (DORT code) was used in [10, 13], the three-dimensional discrete ordinate neutron/photon transport code (TORT version 3) was used in [7], and the three-dimensional Monte Carlo method (MCNP code) was used in [5, 10–12]. In our study, the MCNP5 model was used to estimate the neutron fluxes in different structure components. These fluxes were then used in the ORIGEN2.1 code to calculate the actual activation of the material, taking into consideration the detailed irradiation history. These results were used to prepare the decontamination and dismantling plan for the operational DNRR.

2. History of the DNRR and Its Structural Parameters

The DNRR was originally a 250-kW TRIGA Mark II reactor supplied by General Atomics (USA). The reactor started operations in 1963, and its shutdown was extended from the beginning of 1968 to March 1975. On March 31, 1975, all low-enriched uranium (LEU) TRIGA fuels were removed from the reactor core and then shipped back to the original country, i.e., the USA. During the period 1975–1981, the coolant remained in the reactor pool, but its chemistry quality was not controlled as requested. From 1982 to 1984, under the former Soviet Union's assistance, this reactor was reconstructed, with its thermal power upgraded to 500 kW;

the upgraded reactor was restarted in November 1983 using highly enriched uranium (HEU) fuel fabricated by the former Soviet Union. The reactor serves mainly for radioisotope production, neutron activation analysis, and manpower training [1, 2].

Main parameters of the reactor structure components are summarized in Table 1.

The reactor tank is a cylindrical aluminum tank with an outer diameter of 2.0 m, a height of 6.25 m, and a thickness of 6.0 mm; it is surrounded by a concrete structure for radiation shielding. The reactor core also has a cylindrical form, with a diameter of 44.2 cm and a height of 60.0 cm. For the application of radiation and experimental research, the reactor has 4 horizontal neutron beam tubes, a movable thermal column, and a thermalizing column. The thermal column, with dimensions ($W \times L \times H$) of 1.2 m \times 1.6 m \times 1.2 m, of the former TRIGA reactor remains unchanged. The column has waterproof walls made of aluminum and covered with boron. Graphite blocks with dimensions of 10.2 cm \times 127 cm \times 10.2 cm fill the volume of the column. The outer portion of the column is embedded in the concrete shield; the inner portion is welded to the reactor tank and extends to the outer surface of the graphite reflector. In the vertical plane, the column extends approximately 33.0 cm above and below the graphite reflector, with the centerline coinciding with that of the active core height. The column door is made of heavy concrete. The door has a thickness of 1.3 m and a weight of 17.3 tons and can be removed and inserted on two small rails by an electric motor. The concrete structure of the biological shield for the reactor, which is octagonal-shaped with a width of 6.96 m, a length of 8.63 m, and a height of 6.55 m, has an average density of 2.35 g/cm³, with a density of 3.5 g/cm³ around the thermal column [1, 3]. The layout of the reactor and its main components is presented in Figure 1.

In the reactor, aluminum alloy 6061 of the USA and SAB-1 of the former Soviet Union were made in most structural materials (core support structure, in-core irradiation channels, rotary rack, graphite reflector cover, extracting well, detector housing, neutron beam tubes, etc.). These alloys have very low impurity compositions ($Co \leq 0.003\%$, $Li \leq 0.008\%$ by mass) [14].

3. Methods and Model of Calculation

3.1. Methods and Computer Codes. Calculation of radioactivity in the structural components of the DNRR is difficult

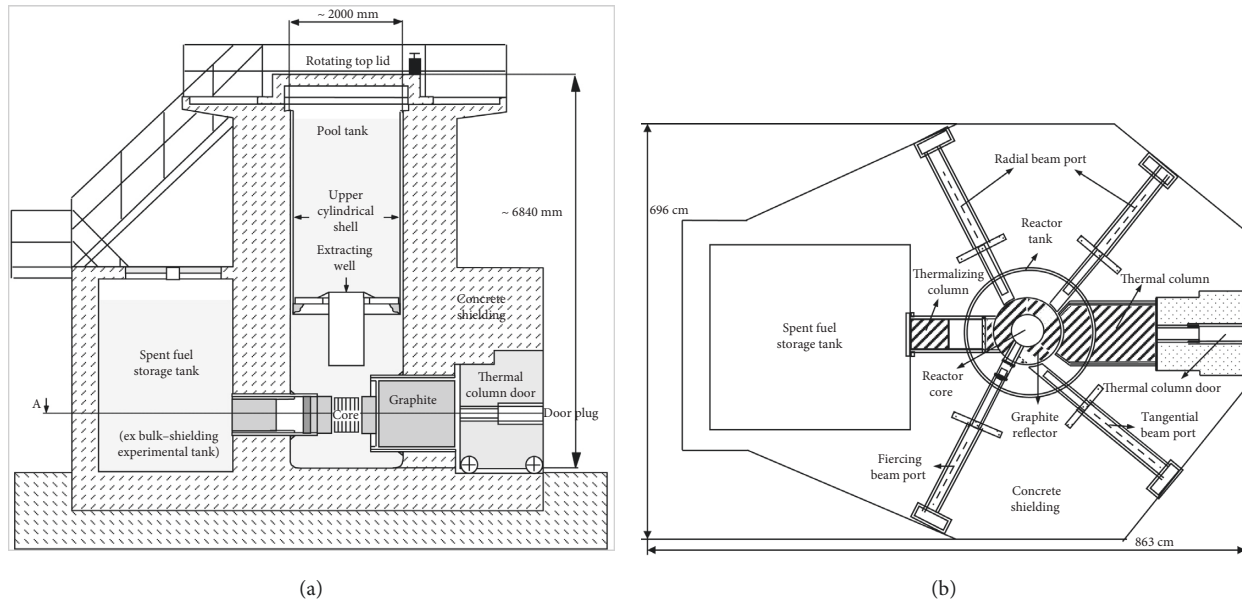


FIGURE 1: Vertical (a) and horizontal (b) section views of the DNRR structure components.

because of the complexity of the geometry, the uncertainty of the material compositions, and operational history data. In general, the geometric structure of the DNRR is the same as that of the TRIGA Mark II type reactor with the existence of different beam ports and thermal and thermalizing columns, which increases the asymmetry, and the neutron flux distribution varies significantly from one location to another. This asymmetry makes the calculation more difficult because each specific location needs to be accounted for.

To obtain the radioactivity in the structural components of the reactor, the material compositions, which generate activated products with long life, were selected to first calculate the activity inventory. Next, the neutron energy spectrum, the density of the neutron flux, and the cross section or reaction rate of elements were calculated. Finally, taking into account the history of reactor operation, the process-generating activated products were determined.

The neutron energy spectrum and activation cross section were obtained using the MCNP5 code [15]. This computer code is a general-purpose, generalized geometry, time-dependent, continuous energy, coupled neutron-photon-electron Monte Carlo transport code. The MCNP5 code deals with the energy range from 10^{-11} MeV to 20.0 MeV for neutrons and from 2.0 keV to 1000 MeV for photons and electrons. ORIGEN2.1 code was used to calculate the activity of activated products in the structural materials of the reactor. The ORIGEN2.1 is a revised version of ORIGEN and incorporates updates to the reactor model, cross sections, fission product yields, decay data, decay photon data, and source code [16]. The ORIGEN2.1 code uses a matrix exponential method to solve a large system of coupled linear, first-order ordinary differential equations with constant coefficients. As the original libraries of ORIGEN2.1 are not suitable for research reactors, the activation cross sections of material compositions in the

reactor were determined by the MCNP5 code. The flowchart of the calculation procedure is shown in Figure 2.

3.2. Model of Calculation. The three-dimensional calculated model for the entire DNRR structures, such as the reactor core, the aluminum, graphite, and concrete components, was basically described as their real geometry. Asymmetric locations around the horizontal neutron beam tubes and thermal column were of particular interest because their activities are fairly high in comparison with other locations. Two-dimensional cross sections of the MCNP5 geometry are shown in Figure 3 for the model with vertical and horizontal cross sections of the concrete shielding, four neutron beam tubes, and thermal column, and Figure 4 shows the model for vertical and horizontal cross sections of the reactor core and graphite reflector.

The cross sections used for MCNP5 calculation were selected from the END/B-VII.1 library. The neutron spectral densities and activation cross sections at nominal power condition and at different locations in the structural components of the reactor were also calculated by the MCNP5 code. Since the ORIGEN2.1 is a zero-dimensional code, all effects on the activation cross sections due to differences in neutron energy spectra at different locations were taken into account in the three-dimensional model of MCNP5.

The irradiated time of structural components of the reactor or the time of reactor operation at the nominal power was assumed to be 45 years from 1984 with 1200 hours each year. As the operation history of the DNRR is complicated, only the last one year was described in detail (12 cycles per year, two weeks of operation, and two weeks of shutdown for each cycle) [17]. The previous operation time was modeled as 1200 hours continuously for each year, with the rest time taken as the shutdown time. To confirm the precise calculation results in the MCNP5, the $1 - \sigma$ statistical uncertainty

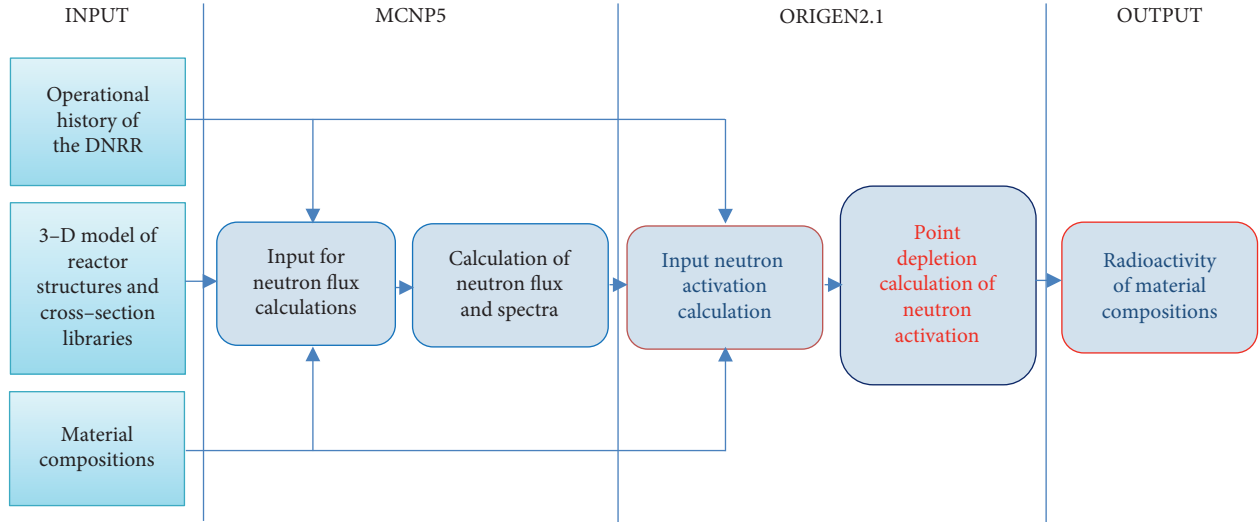


FIGURE 2: Flowchart of the calculation procedure.

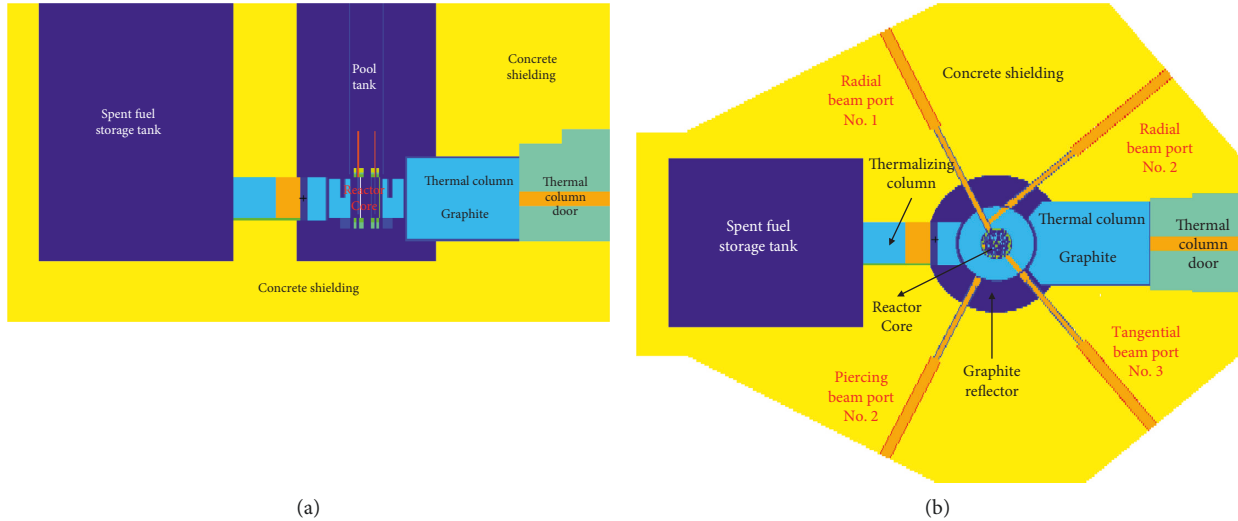


FIGURE 3: Vertical (a) and horizontal (b) cross sections of the MCNP5 geometry with concrete shielding, four neutron beam tubes, and thermal column.

of the integral simulated results for neutron flux and neutron flux distribution was reached within 3% while using the kcode option with total 200 million particles in the problem.

3.3. *Experimental Method.* The neutron flux density and neutron flux distribution at the irradiation positions were measured using the foil activation method. The reaction rate of a thin foil during activation is expressed by the following equation:

$$R = \Phi \cdot \sigma_{\text{act}}, \quad (1)$$

where Φ is neutron flux and σ_{act} is the microscopic activation cross section.

The thermal neutron flux values were measured using bare and cadmium-covered gold foils and were calculated by the following equation [18]:

$$\Phi_{th} = \frac{2 \cdot A \cdot e^{-\lambda \tau}}{\sqrt{\pi} N_A \alpha \sigma_{0, \text{act}} G_{th} (1 - e^{-\lambda \tau})} \sqrt{\frac{T_n}{T_0} \left[\frac{A_b(T, \tau)}{m_b} - \frac{A_{Cd}(T, \tau)}{m_{Cd}} \right]}, \quad (2)$$

where m_b is the mass of bare gold foil (g), m_{Cd} is the mass of cadmium cover (g), T is irradiation time (s), τ is cooling time after irradiation (s), t_m is real time measurement (s), $t_{m, \text{eff}}$ is effective time measurement (s), λ is decay constant of nuclide compound (s^{-1}), η is counting efficiency of detector, γ is gamma abundance factor, α is isotope enrichment, G_{th} is

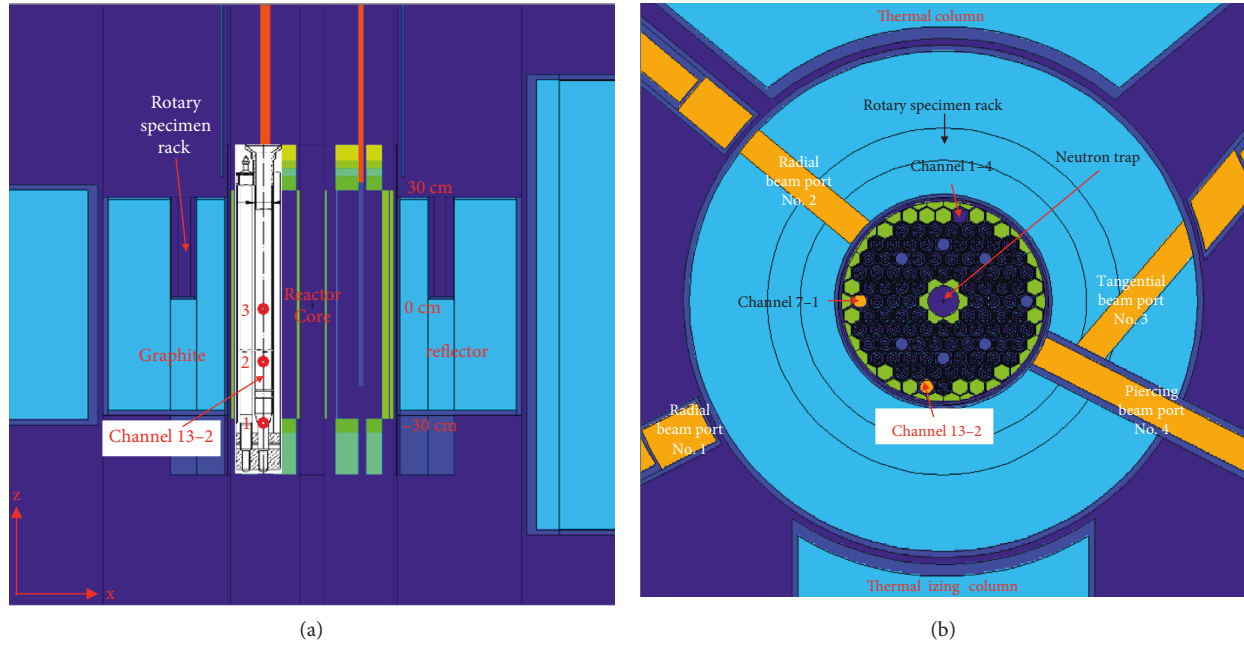


FIGURE 4: Vertical (a) and horizontal (b) cross sections of the reactor core and graphite reflector.

TABLE 2: Thermal neutron flux in the vertical and horizontal irradiation channels of the reactor.

Irradiation channel	Thermal neutron flux (n/cm ² .s)		Discrepancy (%)
	Calculation	Experiment	
Neutron trap	2.21×10^{13}	$(2.10 \pm 0.13) \times 10^{13}$	5.2
Channel 7-1	6.70×10^{12}	$(6.28 \pm 0.58) \times 10^{12}$	6.7
Channel 13-2	6.47×10^{12}	$(6.05 \pm 0.52) \times 10^{12}$	6.9
Rotary specimen rack	4.25×10^{12}	$(4.09 \pm 0.31) \times 10^{12}$	3.8
Thermal column	6.92×10^{10}	$(6.45 \pm 0.70) \times 10^{10}$	6.8
Beam port no. 4	2.45×10^{12}	$(2.33 \pm 0.48) \times 10^{12}$	4.9

thermal neutron self-shielding factor, N_A is Avogadro constant, A is atomic number of isotope, G is ratio of isotope in foil, T_n is neutron temperature (K), T_0 is room temperature (293 K), A_b is activity of bare foil, and A_{Cd} is activity of cadmium cover.

The activity at time τ after finishing the irradiation was calculated by the following equation [6]:

$$A_m \lambda (t_a, \tau) = A_i (1 - e^{-\lambda t_a}), \quad (3)$$

where A_m is the measured activity and A_i is the actual activity at the start of the measurement.

4. Calculated Results of Activity and Volume/Mass of Waste

4.1. Validation of the Computer Codes and Calculation Method. The MCNP5 code and calculation method were validated by comparing the calculation results with the experimental data of neutron flux at the vertical irradiation channels in the reactor core as shown in Table 2 and Figure 4. The calculated values of the maximum thermal flux

($E < 0.625$ eV) at the neutron trap in the core center, at the vertical channels 7-1 and 13-2 in the core periphery, at the rotary specimen rack, at the thermal column, and at the beam port No. 4 were in good agreement with the experimental results, with the maximum discrepancy less than 7%.

The ORIGEN2.1 code and calculation method were validated by comparing the calculation results with the experimental data of impurity radioactivity in three aluminum samples taken from different positions (-32.5 , -17.5 , and -2.1 cm from the core bottom) of the aluminum guiding tube in the irradiation channel 13-2 of the reactor core. This tube was installed on March 9, 1985, and removed on December 9, 2005. As a result, the total irradiation time of the samples was about 249,000 hours based on the reactor operation time of about 100 hours per cycle and 12 cycles per year. Specific activities of the samples were measured by the HPGe gamma spectrometer, where ^{60}Co isotope is the main long-lived activated product as shown in Table 3. The errors in specific activities of ^{60}Co , ^{63}Ni , ^{55}Fe , and ^{59}Ni isotopes evaluated using the ORIGEN2.1 code were each less than 3%. The discrepancy in the calculated and experimental results of the specific activity of ^{60}Co was between 25% and 33%,

TABLE 3: Activity of ^{60}Co isotope in the guiding tube of irradiation channel 13-2.

Samples	Position in aluminum tube (cm)	^{60}Co specific activity (Bq/g)		Discrepancy (%)
		Calculation	Experiment	
1	-32.5	2.77×10^4	$(1.86 \pm 0.17) \times 10^4$	33
2	-17.5	1.35×10^5	$(9.99 \pm 0.19) \times 10^4$	26
3	-2.1	1.71×10^5	$(1.28 \pm 0.16) \times 10^5$	25

TABLE 4: Neutron flux distribution ($\times 10^{12}$ n/cm 2 .s) in the graphite reflector.

z axis (cm)	Distance from the reactor core (cm)							
	24	28	32	35	39	43	47	51
25.0	3.74	3.26	*	*	1.78	1.52	1.22	0.99
7.5	5.27	4.44	3.48	2.90	2.45	2.03	1.73	1.37
-7.5	5.31	4.45	3.36	2.86	2.51	2.10	1.77	1.40
-25.0	3.97	3.41	2.71	2.31	1.96	1.59	1.32	1.07

(*) Rotary specimen rack position.

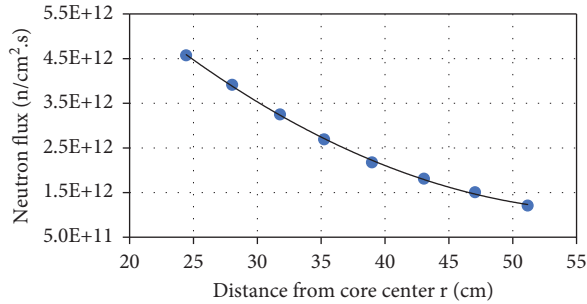


FIGURE 5: Average neutron flux distribution in the graphite reflector.

which is acceptable to be used for developing the decommissioning plan, due to an uncertainty of the reactor geometry, the reactor operation time, and especially the mass of impurity ^{59}Co isotope of the DNRR, in which the uncertainty of the impurity mass can contribute up to 20%. The maximum acceptable discrepancy was estimated to be about 40%.

4.2. Calculated Results of Neutron Flux Distribution. The calculated results for thermal neutron flux distribution in the graphite reflector of the reactor at a nominal power of 500 kW are shown in Table 4 and Figure 5. The average neutron flux at 51 cm from the reactor core center was 1.21×10^{12} n/cm 2 .s, which was about 4 times less than that (4.57×10^{12} n/cm 2 .s) at 24 cm from the core center.

The calculated thermal neutron flux distributions at different locations in the structural components of the reactor at a nominal power of 500 kW are shown in Figure 6. The maximum calculated neutron flux value was 2.21×10^{13} n/cm 2 .s at the core center and 1.23×10^{11} n/cm 2 .s in the graphite block close to the reactor reflector. There were many scattered neutrons at the exit of the four horizontal beam ports and the thermal column due to the installation of neutron collimation tubes inside them for

guiding neutron beams out to the experimental facilities. In fact, these areas had been simulated as air.

4.3. Calculated Results of Activity and Volume/Mass. Figure 7 shows the activity inventory of long-lived nuclides in the shielding structure for 45 years of irradiation time and up to 10 years of cooling. The activity of ^{152}Eu isotope is high; it decays mainly by electron capture and has a half-life of 13.5 years. The activity of ^{55}Fe is relatively high; it decays by electron capture too, emitting X-ray, and has a half-life of 2.7 years. The activity of ^{41}Ca is relatively high too, and its half-life is 9.94×10^4 years; it emits no γ rays. This isotope is generated mostly by a neutron capture reaction (n, γ) from its parent isotope ^{40}Ca , which is the major natural isotope of calcium and is found in all types of concrete [5]. Similarly, the activity of ^{60}Co is relatively high, and its half-life is 5.27 years; it emits two γ rays with high energies of 1.17 and 1.32 MeV. It can be concluded that ^{41}Ca , ^{55}Fe , ^{60}Co , and ^{152}Eu are the four main long-lived isotopes that determine the quantity of activated shielding concrete for preparing the decommissioning plan of the DNRR.

Figure 8 shows the activity inventory of long-lived nuclides in the graphite for 45 years of irradiation time and up to 50 years of cooling. It can be seen that ^{60}Co and ^{152}Eu are the main long-lived isotopes that determine the quantity of activated graphite in the reactor reflector and the thermal and thermalizing columns for preparing the decommissioning plan of the reactor.

Figures 9(a) and 9(b) show the activity inventory of long-lived nuclides in the aluminum of the reactor reflector and the rest of the reactor, respectively, for 45 years of irradiation time and up to 10 years of cooling. The activity of ^{63}Ni is relatively high, and its half-life is 100.1 years. ^{63}Ni isotope mainly generates beta-rays with an energy of 0.067 MeV, so it can be concluded that ^{60}Co and ^{63}Ni isotopes are the main long-lived isotopes that determine the quantity of activated aluminum in the reactor for preparing its decommissioning plan.

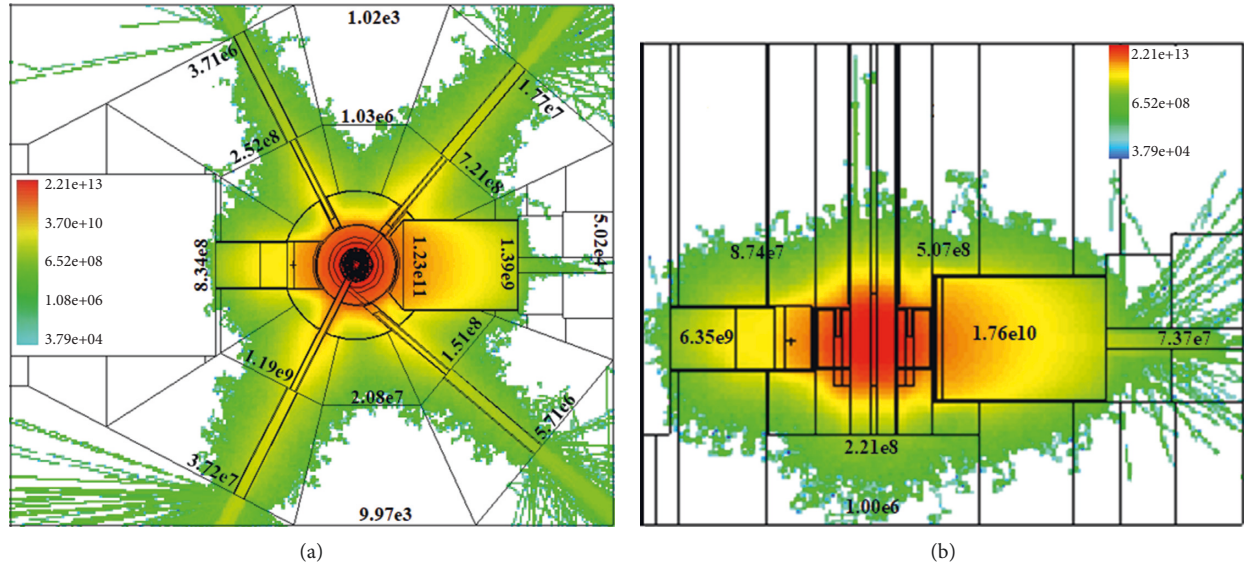


FIGURE 6: MCNP-simulated total neutron fluence rates: thermal neutron flux distribution ($n/cm^2.s$) in the horizontal (a) and vertical (b) cross sections of the reactor.

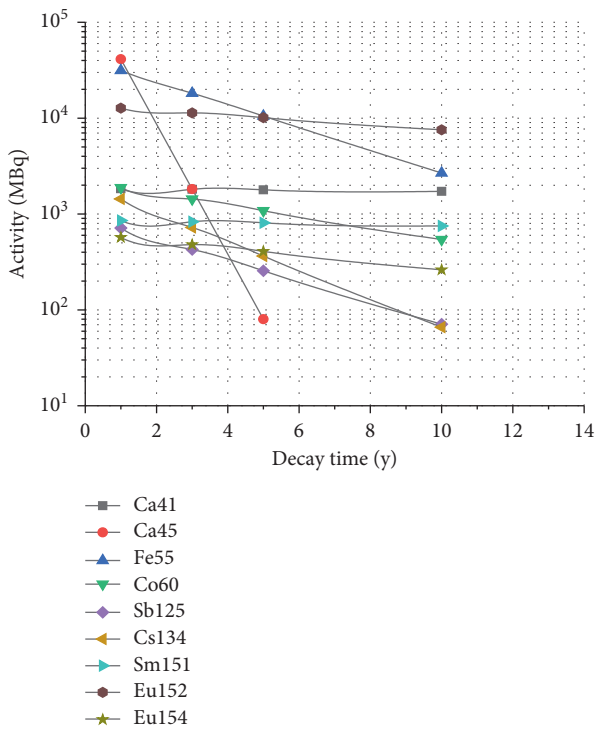


FIGURE 7: Activity of long-lived nuclides in the biological shield structure.

Figure 10 shows the distribution of the specific radiation activity in the reactor shielding and graphite reflector right after reactor shutdown. The highest specific radiation activities of the reactor shielding and graphite reflector are 0.8×10^4 Bq/g and 1.1×10^5 Bq/g, respectively.

The calculated specific activity and volume/mass of the main material components (except for stainless steel which constitutes only a small part of the DNRR) are shown in

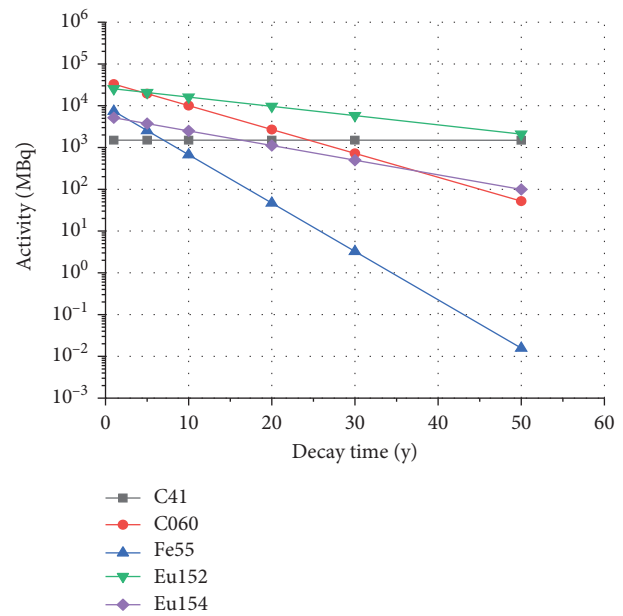


FIGURE 8: Activity of long-lived nuclides in the graphite with the decay time up to 50 years.

Tables 5–8 for two levels of specific activity (>1 Bq/g and >10 Bq/g, according to the “clearance levels” of 1 Bq/g and 10 Bq/g for all isotopes [6, 19]) depending on the decay time of 1, 3, 5 and 10 years. At the specific activity level of >1 Bq/g, the volume of the concrete structure was 46.2 m^3 , with a total activity of 97421.0 MBq after 1 year of decay time. This value reduced to 36.0 m^3 after 5 years and to 31.8 m^3 after 10 years; their total activities after these years were 22821.6 and 12591.1 MBq, respectively, as seen in Table 5.

There were 770 kg of graphite and 129 kg of aluminum in the reflector surrounding the reactor core; therefore, their specific activities were high (thousands of Bq/g for graphite

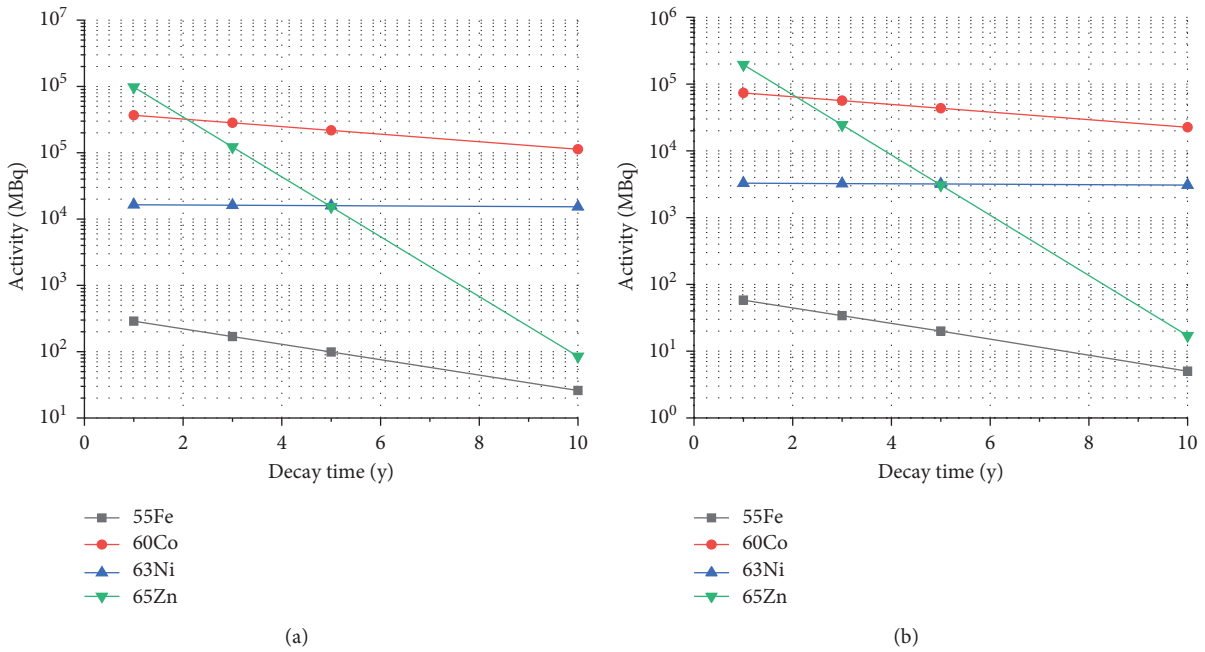


FIGURE 9: (a) Activity of long-lived nuclides in aluminum of the reactor reflector and (b) activity of long-lived nuclides in aluminum of the rest of the reactor.

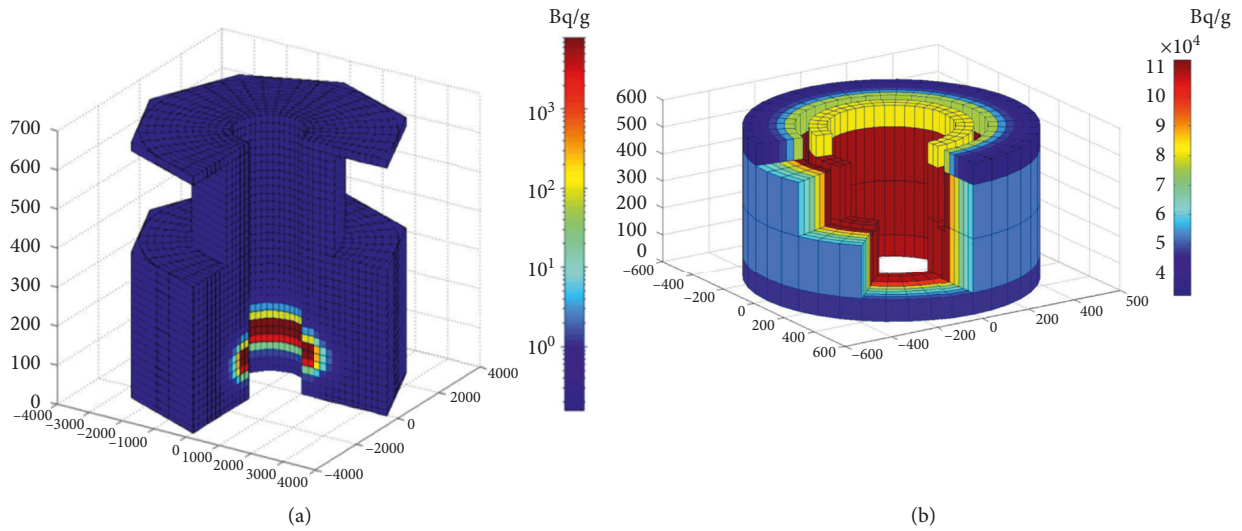


FIGURE 10: Distribution of the specific radiation activity in the reactor shielding (a) and graphite reflector (b) after reactor shutdown.

TABLE 5: Activity of concrete in the reactor concrete structure.

Decay time (years)	Specific activity > 1 Bq/g			Specific activity > 10 Bq/g		
	Volume (m^3)	Specific activity (MBq/m^3)	Total activity (MBq)	Volume (m^3)	Specific activity (MBq/m^3)	Total activity (MBq)
1	46.2	2108.7	97421.0	26.5	3140.2	83215.3
3	38.4	894.0	34328.6	20.1	1638.1	32925.8
5	36.0	633.9	22821.6	18.0	1258.9	22660.2
10	31.8	395.9	12591.1	14.5	852.3	12358.4

TABLE 6: Activity of graphite and aluminum in the reactor reflector.

Decay time (years)	Specific activity > 1 Bq/g			Specific activity > 1 Bq/g		
	Graphite mass (kg)	Specific activity (Bq/g)	Total activity (MBq)	Aluminum Mass (kg)	Specific activity (Bq/g)	Total activity (MBq)
1	770	7.95E+04	6.12E+04	129	1.36E+06	1.76E+05
3		5.95E+04	4.58E+04		4.22E+05	5.44E+04
5		4.82E+04	3.71E+04		2.49E+05	3.21E+04
10		3.09E+04	2.38E+04		1.28E+05	1.66E+04

TABLE 7: Activity of graphite in the thermal and thermalizing columns.

Decay time (years)	Specific activity > 1 Bq/g			Specific activity > 10 Bq/g		
	Mass (kg)	Specific activity (Bq/g)	Total activity (MBq)	Mass (kg)	Specific activity (Bq/g)	Total activity (MBq)
1	5763	9.13E+02	5264	3850	1.37E+03	5275
3	5763	7.18E+02	4140	3731	1.08E+03	4020
5	5721	5.98E+02	3421	3608	8.97E+02	3237
10	4907	4.04E+02	1982	3084	6.06E+02	1868

TABLE 8: Activity of aluminum in the reactor components (except in the reflector).

Decay time (years)	Specific activity > 1 Bq/g			Specific activity > 10 Bq/g		
	Mass (kg)	Specific activity (Bq/g)	Total activity (MBq)	Mass (kg)	Specific activity (Bq/g)	Total activity (MBq)
1	580	2.67E+05	154932	540	2.71E+05	146250
3	570	8.95E+04	50992	480	9.07E+04	43529
5	565	5.84E+04	32984	461	5.84E+04	26912
10	541	5.68E+04	30729	412	5.68E+04	23402

and hundreds of thousands of Bq/g for aluminum, as seen in Table 6). The total activities of the reflector graphite were 6.12×10^4 , 3.71×10^4 , and 2.38×10^4 MBq after a decay time of 1 year, 5 years, and 10 years, respectively. The total activities of the aluminum structure in the reactor reflector after 1 year, 5 years, and 10 years of decay time were 1.76×10^5 , 3.21×10^4 , and 1.66×10^4 MBq, respectively.

Although the graphite constituents in other components besides the reflector, such as the thermal and thermalizing columns, were so large in mass (estimated about 5763 kg, as seen in Table 7), their specific activities were very low, and therefore, their total activities were much lower than that in the reflector.

The aluminum constituents in other components besides the reflector were also fairly large. The mass of waste at the specific activity level of >1 Bq/g and a decay time of 1 year after reactor shutdown was 580 kg, and its total activity was 154932 MBq. This value reduced to 565 kg after 5 years and 541 kg after 10 years; their total activities after these years were 32984 MBq and 30729 MBq, respectively, as seen in Table 8.

5. Conclusion

The radioactivity inventory and volume/mass of radioactive waste of the structural components of the DNRR were determined and estimated, respectively. For modeling, the neutron fluxes and energy spectra at different locations of the structural components, as well as the activation cross sections of the interest isotopes, were calculated using the

MCNP5 code. Based on the activation cross sections and neutron fluxes at different locations of the structural components, in combination with the history of reactor operation, the activities in the structural components of the reactor were determined using the ORIGEN2.1 code.

The activity inventories of the main long-lived nuclides in the biological shielding structure were determined. The results showed that ^{41}Ca , ^{55}Fe , ^{60}Co , and ^{152}Eu are the four main long-lived isotopes for determining the quantity of activated shielding concrete, ^{60}Co and ^{152}Eu are the main long-lived isotopes for determining the quantity of activated graphite in the reactor reflector and thermal and thermalizing columns, and ^{60}Co and ^{63}Ni are the main long-lived isotopes for determining the quantity of activated aluminum.

The volume/mass of radioactive waste in the structural components of the DNRR was estimated. For 10 years of cooling time, the results showed that the main radioactive waste for decommissioning planning comes from activated shielding concrete, graphite, and aluminum. The volume and total activity of activated shielding concrete were 31.8 m^3 and 12591.1 MBq, respectively, at the "clearance level" of 1 Bq/g, whereas the corresponding values at the "clearance level" of 10 Bq/g were 14.5 m^3 and 12358.4 MBq, respectively. The mass and total activity of activated graphite in the reflector at "clearance level" of 1 Bq/g were 770 kg and 2.38×10^4 MBq, respectively, while the corresponding values for activated aluminum at the same "clearance level" were 129 kg and 1.66×10^4 MBq, respectively. For activated graphite in the thermal and thermalizing columns, the mass

and total activity at the “clearance level” of 1 Bq/g were 4907 kg and 1982 MBq, respectively, while the corresponding values at the “clearance level” of 10 Bq/g were 3084 kg and 1868 MBq, respectively. The mass and total activity of activated aluminum in the reactor components at “clearance level” of 1 Bq/g were 541 kg and 30729 MBq, respectively, while the corresponding values at the “clearance level” of 10 Bq/g were 412 kg and 23402 MBq, respectively.

The obtained results have been used to update the decontamination and dismantling plan of the DNRR with a 15-chapter format following the IAEA guideline [20].

Data Availability

Data will be made available upon request.

Conflicts of Interest

The authors declare that they have no conflicts of interest regarding the publication of this paper.

Acknowledgments

The authors are grateful to the administrative staffs of DNRI for their kind support. The staffs at Reactor Physics and Engineering Department of DNRI are acknowledged for their valuable technical discussions. This research was supported by the Ministry of Science and Technology of Vietnam under Grant no. DTCT.05/20/VNCHN.

References

- [1] Nuclear Research Institute, *Safety Analysis Report for the Dalat Nuclear Research Reactor*, Nuclear Research Institute, Dalat, 2018.
- [2] K.-C. Nguyen, V. V. Le, T. N. Huynh, B.-V. Luong, and N.-D. Nguyen, “Steady-state thermal-hydraulic analysis of the LEU-fueled Dalat nuclear research reactor,” *Science and Technology of Nuclear Installations*, vol. 2021, Article ID 6673162, 10 pages, 2021.
- [3] K.-C. Nguyen, V. V. Le, T. N. Huynh, B.-V. Luong, N.-D. Nguyen, and H.-N. Tran, “Interim storage of the Dalat nuclear research reactor: radiation safety,” *Science and Technology of Nuclear Installations*, vol. 2021, Article ID 7327045, 10 pages, 2020.
- [4] International Atomic Energy Agency, “Decommissioning of nuclear power plants, research reactors and other nuclear fuel cycle facilities,” IAEA, Vienna, Specific Safety Guide, No. SSG-47, 2018.
- [5] T. Zagar and M. Ravnik, “Determination of long-lived neutron activation products in reactor shielding concrete samples,” *Nuclear Technology*, vol. 140, no. 1, pp. 113–126, 2002.
- [6] M. Lezar, T. Zagar, and M. Ravnik, “Estimation of waste volumes after TRIGA Mark II research reactor dismantling,” in *Proceedings of the International Conference Nuclear Energy for New Europe 2003*, Portoroz, Slovenia, September 2003.
- [7] T. Zagar, M. Bozic, and M. Ravnik, “Long-lived activation products in TRIGA Mark II research reactor concrete shield: calculation and experiment,” *Journal of Nuclear Materials*, vol. 335, no. 3, pp. 379–386, 2004.
- [8] I. E. Stamatelatos, F. Tzhika, S. Valakis, and A. Hanousis, “Dose assessment for decommissioning planning of the Greek research reactor primary cooling system,” *International Nuclear Safety Journal*, vol. 3, no. 4, pp. 37–42, 2014.
- [9] G. Toth, “Initial decommissioning planning for the Budapest research reactor,” *Nuclear Technology & Radiation Protection*, vol. 26, no. 1, pp. 92–99, 2011.
- [10] G. Hampel, F. Scheller, W. Bernnat, G. Pfister, U. Klauz, and E. Gerhards, “Calculation of the activity inventory for the TRIGA reactor at the medical university of hannover (MHH) in preparation for dismantling the facility,” in *Proceedings of the Waste Management Conference (WM’02)*, Tuscon, Arizona, USA, February 2002.
- [11] A. Rätty, T. Lavonen, A. Leskinen et al., “Characterization measurements of Fluenta and Graphite in FiR1 TRIGA research reactor decommissioning waste,” *Nuclear Engineering and Design*, vol. 353, Article ID 110198, 2019.
- [12] A. Rätty and P. Kotiluoto, “FIR 1 TRIGA activity inventories for decommissioning planning,” *Nuclear Technology*, vol. 194, no. 1, pp. 28–38, 2016.
- [13] E. Ionescu, D. Gurau, S. Doru, and O. G. Dului, “Decommissioning of the VVR-S research reactor-radiological characterization of the reactor block,” *Romanian Reports in Physics*, vol. 64, no. 2, pp. 387–398, 2012.
- [14] Nuclear Research Institute, *The Determination of Impurities Which Generate Activated Products with Long-Life in Structural Materials of the Dalat Reactor*, Reactor Center, Vietnam, 2010.
- [15] *X-5 Monte Carlo Team, MCNP - A General Monte Carlo N-Particle Transport Code, Version 5*, Los Alamos National Laboratory, New Mexico, USA, 2005.
- [16] A. G. Croff, *A User Manual for the ORIGEN2 Computer Code*, Oak Ridge National Laboratory, Oak Ridge, Tennessee, 1980.
- [17] Dalat Nuclear Research Institute, *Operational Workbook of the Dalat Research Reactor*, Dalat Nuclear Research Institute, Dalat, Vietnam, 1984–2021.
- [18] International Atomic Energy Agency, *Regional Training Course on Calculation and Measurement of Neutron Flux Spectrum for Research Reactors*, Serpong, Indonesia, 1993.
- [19] International Atomic Energy Agency, *Clearance Levels for Radionuclides in Solid Materials. Application of Exemption Principles IAEA-TECDOC-855*, IAEA, Vienna, 1996.
- [20] International Atomic Energy Agency, “Standard format and content for safety related decommissioning documents,” Safety Report Series, No. 45, IAEA, Vienna, 2005.